Quantum Walks for Chemical Reaction Networks

Seenivasan Hariharan,[1,2,3] Sebastian Zur,[4,a)] Sachin Kinge,[5] Lucas Visscher,[6] Kareljan Schoutens,[1,2] and Stacey Jeffery[2,7]

[1)] *Institute of Theoretical Physics, University of Amsterdam, Amsterdam, The Netherlands*

[2)] *QuSoft, CWI, Amsterdam, The Netherlands*

[3)] *Quantum Application Lab, Startup Village, Amsterdam, The Netherlands*

[4)] *IRIF & CNRS, Paris, France*

[5)] *Toyota Motor Europe, Materials Engineering Division, Hoge Wei 33, B-1930 Zaventum, Belgium*

[6)] *Theoretical Chemistry, Vrije Universiteit, De Boelelaan 1083, NL-1081 HV, Amsterdam, The Netherlands*

[7)] *KdVI, University of Amsterdam, Amsterdam, The Netherlands*

We lay the foundation for a quantum algorithmic framework to analyse fixed-structure chemical reaction networks (CRNs) using quantum random walks (QRWs) via electrical circuit theory. We model perturbations to CRNs, such as, species injections that shift steady-state concentrations, while keeping the underlying species-reaction graph fixed. Under physically meaningful mass-action constraints, we develop quantum algorithms that (i) decide reachability of target species after perturbation, (ii) sample representative reachable species, (iii) approximate steady-state fluxes through reactions, and (iv) estimate total Gibbs free-energy consumption. Our approach offers new tools for analysing the structure and energetics of complex CRNs, and opens up the prospect of scalable quantum algorithms for chemical and biochemical reaction networks.

[a)] The majority of this work was conducted while SZ was affiliated with CWI & QuSoft, the Netherlands.

I. INTRODUCTION

Chemical reaction networks (CRNs), models of interacting chemical species connected by reaction rules, provide an abstract framework for modeling how molecular species interact through chemical transformations in complex chemical and biochemical processes [1]. CRNs are prominent in the fields of catalysis [2], atmospheric chemistry [3], and biochemistry [4], to name a few. In these fields, CRN-based computational models are essential to reveal short-lived intermediates, reaction mechanisms of elementary reactions, and the overall reaction pathways. CRN research broadly falls into two areas: generation (or exploration) of the networks [5], and their analysis [6]. While recent advances have automated the construction of large-scale CRNs [5, 7–10], extracting meaningful insight from them remains a significant challenge.

Perturbations to a CRN can affect its behaviour differently depending on whether its structure is fixed or variable. We focus on fixed-structure CRNs, defined by a finite set of species, e.g. $\{A, B, C, D\}$, and a finite set of reactions between these species, e.g. $A \to 2B, A + C \to D$. Here, the species-reaction graph remains unchanged and perturbations alter only concentrations or external fluxes. Even within this framework, injecting species can shift steady states and activate alternative pathways, increasing the system's effective dimensionality and coupling [11, 12]. Such effects undermine classical algorithms that exploit sparsity or local independence, rendering the analysis of large CRNs computationally challenging despite a fixed underlying network [6, 13].

One of the most prominent models to study the interactions in an abstract CRN is *mass action kinetics* [1]. This continuous and deterministic model governs the dynamics of the reactions in the CRN through differential equations and works well in the regime where the total number of molecules is high. Under standard assumptions on the mass action kinetics and the structure of the CRN, the resulting dynamics give rise to a natural thermodynamic interpretation of the system. In particular, the system's evolution can often be associated with the dissipation of a free energy–like function, and its steady states correspond to thermodynamic equilibria where no net change in species concentrations occurs.

Many state-of-the-art approaches analyse a CRN by viewing it as a directed weighted graph, but there is a large degree of freedom as to how the mass action kinetics are encoded in this graph, as seen by the various approaches in the literature [2, 5, 6, 8, 13–36]. These

representations allow the CRN to describe a wide range of systems in chemistry, biology, and engineering. However, since the mass action kinetics are typically modeled by non-linear differential equations, they are often analytically intractable and computationally challenging to simulate or reason about [6, 37–40]. Different strategies are employed to circumvent this problem, by relaxing different aspects of the problem at hand (see Section A).

A. Contributions

By levering the connection between CRNs and electrical circuit theory [41, 42] and quantum walks and random walks on electrical networks [43, 44], we expose a novel and direct connection between CRNs and *quantum walk algorithms*, tying the mass-action dynamics of a CRN to the parameters in quantum walk algorithms. We use this connection to design quantum walks that probe both structural and dynamical properties of the CRN. Assuming a set of natural and physically meaningful constraints on the mass-action system, and given access to all thermodynamic quantities with respect to the equilibrium, we develop quantum algorithms that: (i) decide whether a given set of target species is reachable under a injection of species in the system, denoted by η; (ii) return a representative target species, conditioned on reachability; (iii) approximate the net steady-state flux $J_r(c)$ through any reaction r in the CRN, where c is the new concentrations vector induced by the injection η; and (iv) approximate the total Gibbs free-energy consumption $\Phi(c)$.

From a purely quantum algorithmic perspective, we prove new insights in the setting of *multidimensional quantum walks*, the most recent and powerful design paradigm for quantum walk algorithms [45–47]. We exhibit a novel use case of *alternative neighbourhoods*, showing how they can be leveraged to sample from specific electrical flow states if certain graph theoretic constraints are met.

B. Discussion

While many state-of-the-art algorithms for analysing CRNs employ classical graph primitives like Breadth-First Search, Depth-First Search, or random walks [2, 5, 6, 8, 13–36], a formal computational cost analysis has been largely absent from the literature. This is primarily because a standard computational access model for CRNs has not been established.

For the large-scale networks relevant in practical applications, however, it is reasonable to model access to the CRN's structure and its precomputed thermodynamic properties in a manner analogous to an adjacency matrix. By adopting this perspective and assuming that the network data is stored in readable QRAM, we can leverage quantum walks to achieve a provable speedup over classical methods. For instance, in the adjacency matrix model, quantum walks solve the s-t connectivity problem on an n-vertex graph in $O(n^{3/2})$ queries, whereas classical algorithms require $\Omega(n^2)$ queries [48]. In our context, this problem is directly analogous to determining the reachability of a target species, where n represents the number of species in the CRN. Furthermore, because our computational cost analysis incorporates the CRN's intrinsic thermodynamic quantities, the resulting quantum speedup may be even more pronounced than suggested by bounds based solely on the number of species.

Our analysis is predicated on a set of thermodynamic constraints that the CRN must satisfy. A prominent and practically relevant example of a CRN that meets these requirements is *competitive binding*, where an injected inhibitor species competes with the substrate for binding to an enzyme. This scenario can be represented within the bipartite structure of the CRN by introducing additional species and binding/unbinding reactions, preserving the network topology while modifying the equilibrium composition and flux distribution [49]. From a kinetic standpoint, competitive inhibition increases the apparent Michaelis constant K_M without affecting the maximal velocity $V_{\max}$, as derived under the quasi–steady-state approximation [50, 51]. From the perspective of chemical reaction network theory, the addition of such species corresponds to a structured expansion of the stoichiometric matrix, consistent with the deficiency-based framework [1]. Mechanistic encodings of this type are widely used in systems biology to integrate enzyme regulation into network-level models, ensuring thermodynamic consistency and tractability [52]. Although we do not explicitly model enzyme–inhibitor dynamics here, the structural similarity between CRNs with competitive inhibitors and the bipartite graphs considered in this work suggests that our framework could be useful in analysing such perturbations. More broadly, our results indicate that quantum algorithms for CRNs may provide a scalable approach for studying mechanistic aspects of biochemical regulation, drug action, and energy dissipation in large molecular networks.

II. PRELIMINARIES

A. Graph theory and electrical networks

In this section, we define the necessary graph-theoretic concepts and provide a review of basic knowledge on electrical networks.

Definition II.1 (Network)**.** *A network is a connected weighted graph $G = (V, E, \mathsf{w})$ with a vertex set V, an (undirected) edge set E and some weight function $\mathsf{w} : E \to \mathbb{R}_{>0}$. Since edges are undirected, we can equivalently describe the edges by some set $\overrightarrow{E}$ such that for all $\{u, v\} \in E$, exactly one of (u, v) or (v, u) is in $\overrightarrow{E}$. The choice of edge directions is arbitrary. Then we can view the weights as a function $\mathsf{w} : \overrightarrow{E} \to \mathbb{R}_{>0}$, and for all $(u, v) \in \overrightarrow{E}$, define $\mathsf{w}_{v,u} = \mathsf{w}_{u,v}$. For convenience, we define $\mathsf{w}_{u,v} = 0$ for every pair of vertices such that $(u, v) \notin E$. We write*

$$\mathsf{W} := \sum_{(u,v)\in\overrightarrow{E}} \mathsf{w}_{u,v},$$

for the total weight of the network.
For an implicit network G, and $u \in V$, we will let $\Gamma(u)$ denote the neighbourhood *of u:*

$$\Gamma(u) := \{v \in V : \{u, v\} \in E\}.$$

We use the following notation for the out- and in-neighbourhoods *of $u \in V$:*

$$\begin{aligned} \Gamma^+(u) &:= \{v \in \Gamma(u) : (u, v) \in \overrightarrow{E}\} \\ \Gamma^-(u) &:= \{v \in \Gamma(u) : (v, u) \in \overrightarrow{E}\}, \end{aligned} \tag{1}$$

To build intuition from physics and apply results from electrical network theory, it is useful to interpret our networks as *electrical networks*.

Definition II.2 (Electrical network)**.** *Given a network $G = (V, E, \mathsf{w})$ with a weight function w, we can interpret every edge $\{u, v\} \in E$ as a resistor with resistance $1/\mathsf{w}_{u,v}$. This allows G to be modeled as an* electrical network*.*

Definition II.3 (Flow)**.** *A* flow *on a network $G = (V, E, w)$ is a real-valued function on the edges $\theta : E \to \mathbb{R}$, such that $\theta_{u,v} = -\theta_{v,u}$ for every $\{u, v\} \in E$. For any flow f on G and any vertex $u \in V$, we define the net flow leaving u as $\theta_u = \sum_{v\in\Gamma(u)} \theta_{u,v}$. Flow is said to be* conserved *at u if $\theta_u = 0$. A vertex u is called a* source *if $\theta_u > 0$ and a* sink *if $\theta_u < 0$.*

Given a marked set $M \subset V$ *and an* initial probability distribution σ *on* $V \setminus M$*, a* (unit) σ-M flow *is a flow* θ *such that each source* u *is in the support of* σ *and satisfies* $\theta_u = \sigma(u)$*, and each sink is in* M *with* $\sum_{u \in M} \theta_u = -1$*.*

The energy *of a flow* θ *is defined as:*

$$\mathsf{E}(\theta) := \sum_{(u,v) \in \overrightarrow{E}} \frac{\theta_{u,v}^2}{\mathsf{w}_{u,v}}.$$

The effective resistance $\mathsf{R}_{\sigma,M}$ *is the minimal energy* $\mathsf{E}(\theta)$ *over all unit* σ-M *flows* θ*. When* σ *is supported on a single vertex* s*,* M *is supported on a single vertex* t*, or both, we simplify the notation to* $\mathsf{R}_{s,M}$*,* $\mathsf{R}_{\sigma,t}$*, or* $\mathsf{R}_{s,t}$*, respectively. The* σ-M electrical flow *is the unique unit* σ-M *flow that achieves this minimal energy.*

Definition II.4 (Potential)**.** *A* potential vector *(also known as potential function) on a network* $G = (V, E, \mathsf{w})$ *is a real-valued function* $\mathsf{p} : V \to \mathbb{R}$ *that assigns a potential* p_u *to each vertex* $u \in V$*.*

Two fundamental laws governing electrical networks are *Kirchhoff's Law* (also known as Kirchhoff's Node Law) and *Ohm's Law*. Kirchhoff's Law defines an σ-M flow as follows:

Definition II.5 (Kirchhoff's Law)**.** *For any given* σ-M *flow* θ *on an electrical network* $G = (V, E, \mathsf{w})$*, the amount of electrical flow entering any vertex* $u \in V \setminus \{supp(\sigma) \cup M\}$ *must equal the amount of flow exiting* u*. In other words:*

$$\sum_{v \in \Gamma(u)} \theta_{u,v} = 0.$$

Ohm's Law, on the other hand, states that if a unit of current is injected according to the initial probability distribution σ and extracted at the sinks in M of the electrical network G, then an induced potential vector p is generated, as described in Definition II.4, which is related to the σ-M electrical flow θ in the following manner:

Definition II.6 (Ohm's Law)**.** *Let* θ *be the* σ-M *electrical flow on an electrical network* $G = (V, E, \mathsf{w})$*. Then there exists a potential vector* p *such that the potential difference between the two endpoints of any edge* $\{u, v\} \in E$ *is equal to the amount of electrical flow* $\theta_{u,v}$ *along this edge multiplied with the resistance* $1/\mathsf{w}_{u,v}$*, that is,* $\mathsf{p}_u - \mathsf{p}_v = \theta_{u,v}/\mathsf{w}_{u,v}$*.*

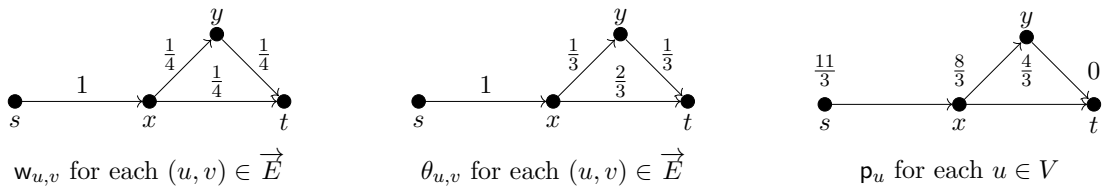

Figure 1. Graph G with its s-t electrical flow θ and corresponding potential p at each vertex.

The potential p induced by an σ-M electrical flow θ in Ohm's Law is not unique. Therefore, it is common practice to consider the potential p that assigns $\mathsf{p}_u = 0$ for every $u \in M$, in which case $\mathsf{p}_u = \sigma(u)\mathsf{R}_{u,M}$ for very $u \in \mathrm{supp}(\sigma)$, where $\mathsf{R}_{u,M}$ is the effective resistance between u and M.

We provide an example graph to help make the above definitions more concrete. Consider the network $G = (V, E, \mathsf{w})$, where the vertex set is given by $V = \{s, x, y, t\}$, and the directed edge set is $\overrightarrow{E} = \{(s,x), (x,y), (x,t), (y,t)\}$. The weight of each edge $(u,v) \in \overrightarrow{E}$ is $\mathsf{w}_{u,v} = \frac{1}{4}$, except for the edge (s,x), which has a weight of $\mathsf{w}_{s,x} = 1$. This network is visualised in Figure 1, along with the s-t electrical flow θ on G and the corresponding potential vector p. It is straightforward to verify that the flow θ satisfies Kirchhoff's Law (see Definition II.5), which states that the net flow entering any vertex, except for the source s and the sink t, is zero. Additionally, the potential vector p satisfies Ohm's Law (see Definition II.6), meaning that for each edge (u,v), the potential difference $\mathsf{p}_u - \mathsf{p}_v$ is given by $\frac{\theta_{u,v}}{\mathsf{w}_{u,v}}$. The effective resistance $\mathcal{R}_{s,t}$ can be determined in two ways: either by computing the energy of the flow depicted in Figure 1, or by noting that the potential at s is $\mathsf{p}_s = \frac{11}{3}$. Thus, the effective resistance for this network is $\mathcal{R}_{s,t} = \frac{11}{3}$.

B. Chemical reaction networks

A chemical reaction network (CRN) provides a mathematical framework for representing and analysing a system of complex chemical reactions. It is particularly useful for studying the kinetics of large reaction networks. In this section, we adopt the definition of a CRN, as well as related notions, as introduced by Feinberg [1].

Definition II.7 (Chemical Reaction Network)**.** *A chemical reaction network (CRN) is a tuple $(\mathcal{S}, \mathcal{C}, \mathcal{R})$, where:*

(i) $\mathcal{S}$ *is a finite set, whose elements are called the species of the network.*

(ii) $\mathcal{C} \subset \mathbb{R}^{\mathcal{S}}_{\geq 0}$ *is a finite set of vectors called the complexes of the network.*

(iii) $\mathcal{R} \subset \mathcal{C} \times \mathcal{C}$ *is a finite set of ordered pairs called* ***reactions****, satisfying the following conditions:*

(a) $\forall y \in \mathcal{C}$, $(y, y) \notin \mathcal{R}$ *(no trivial reactions).*

(b) $\forall y \in \mathcal{C}$, *there exists* $y' \in \mathcal{C}$ *such that either* $(y, y') \in \mathcal{R}$ *or* $(y', y) \in \mathcal{R}$ *(every complex participates in at least one reaction either as a reactant or as a product.*

For a reaction $(y, y') \in \mathcal{R}$, *we denote it by* $y \to y'$, *where* y *is called the reactant complex and* y' *is the product complex.*

As an example, consider the CRN defined by

$$\mathcal{S} = \{A, B, C, D, E\}, \tag{2}$$

$$\mathcal{C} = \{A, 2B, A + C, D, B + E\}, \tag{3}$$

$$\mathcal{R} = \big\{A \to 2B, 2B \to A, A + C \to D, D \to A + C, D \to B + E, B + E \to A + C\big\}. \tag{4}$$

This corresponds to the reaction system whose standard reaction diagram is displayed as

$$\begin{aligned} A &\rightleftharpoons 2B, \\ A + C &\rightleftharpoons D, \\ D &\to B + E, \\ B + E &\to A + C. \end{aligned}$$

A CRN is not just a static system; it also has dynamical relationships between the various complexes. These dynamics are governed by the *kinetics* of the CRN. The kinetics act on a *concentrations vector* $c \in \mathbb{R}^{\mathcal{S}}_{\geq 0}$, whose components c_s (for each $s \in \mathcal{S}$) specify the number of s-molecules per unit volume of the mixture. In this work, we consider the following specific form of kinetics:

Definition II.8 (Mass Action Kinetics)**.** *A* mass action kinetics *for a chemical reaction network* $(\mathcal{S}, \mathcal{C}, \mathcal{R})$ *is an assignment to each reaction* $y \to y'$ *of a* mass action rate function $\mathcal{K}_{y \to y'} \colon \mathbb{R}^{\mathcal{S}}_{\geq 0} \to \mathbb{R}_{\geq 0}$ *such that there exists a positive number* $k_{y \to y'}$ *with*

$$\mathcal{K}_{y \to y'}(c) = k_{y \to y'} \prod_{s \in \mathcal{S}} c_s^{y_s}.$$

Here $k_{y\to y'}$ *is the* rate constant *for the reaction* $y \to y'$*, and the component* y_s *of* y *is the* stoichiometric coefficient *of species* s *in the reactant complex* y*.*

In the above definition of the mass action rate function, we adopt the convention $0^0 = 1$ when a particular concentration c_s is zero. For the CRN in (2), consider, for example, the reaction $A + C \to D$. Then

$$\mathcal{K}_{A+C\to D}(c) = k_{A+C\to D}(c_A)^1(c_B)^0(c_C)^1(c_D)^0(c_E)^0 = k_{A+C\to D}c_A c_C.$$

Similarly, for the reaction $2B \to A$, we have

$$\mathcal{K}_{2B\to A}(c) = k_{2B\to A}(c_B)^2.$$

It is convention to abbreviate

$$\prod_{s\in\mathcal{S}} c_s^{y_s} = c^y,$$

so that the mass action rate functions can be written more succinctly as

$$\mathcal{K}_{y\to y'}(c) = k_{y\to y'}c^y.$$

mass action kinetics for a CRN $(\mathcal{S}, \mathcal{C}, \mathcal{R})$ is completely specified by assigning a positive rate constant $k_{y\to y'}$ to each reaction $y \to y' \in \mathcal{R}$. That is to say, a mass action kinetics is specified by an element $k \in \mathbb{R}_+^{\mathcal{R}}$. We therefore speak of a *mass action system (MAS)* $(\mathcal{S}, \mathcal{C}, \mathcal{R}, k)$, which is the CRN $(\mathcal{S}, \mathcal{C}, \mathcal{R})$ combined with the mass action kinetics uniquely determined by k.

C. The thermodynamics of an MAS

In this section, we delve deeper into the thermodynamics of an MAS, following the notions in [53]. When studying the kinetics of an MAS, it is convenient to study *reversible* reactions. For a CRN $(\mathcal{S}, \mathcal{C}, \mathcal{R})$, we say that a reaction $y \to y' \in \mathcal{R}$ is said to be reversible if $y' \to y \in \mathcal{R}$. For a reversible reaction $y \to y'$, we can define its *net flux* $J_{y\to y'}(c)$ as follows:

$$J_{y\to y'}(c) := \mathcal{K}_{y\to y'}(c) - \mathcal{K}_{y'\to y}(c). \tag{5}$$

This net flux is positive if the reaction proceeds predominantly in the forward direction and negative if the backward direction is dominant. The net flux can also be zero, reflecting a perfect balance of forward and backward processes in that reaction.

If all reactions in $\mathcal{R}$ for a CRN $(\mathcal{S}, \mathcal{C}, \mathcal{R})$ are reversible, we say that the CRN is reversible. To avoid listing both directions of each reversible pair of reaction, we fix a subset $\overrightarrow{\mathcal{R}} \subset \mathcal{R}$ called the set of *oriented reactions*, containing exactly one direction from every reversible pair $y \to y', y \to y' \in \mathcal{R}$, similarly as to how the directed edge set $\overrightarrow{E}$ is obtained from the edge set E in a graph. We can fully characterise the set of reversible reactions $\mathcal{R}$ from just $\overrightarrow{\mathcal{R}}$. If $r = y \to y'$, we use $\overline{r}$ to denote $y' \to y$. This means that, depending on the chosen direction, $J_r(c)$ would change sign.

For a reversible CRN, if the net flux of all reactions is zero, that is, there exists a vector of concentrations $c^* \in \mathbb{R}^{\mathcal{S}}_{\geq 0}$ such that, for each reaction $r \in \overrightarrow{\mathcal{R}}$,

$$\mathcal{K}_r(c^*) = \mathcal{K}_{\overline{r}}(c^*), \tag{6}$$

then we say that the MAS is in *detailed balance*. Such a vector c^* is often referred to as a (thermodynamic) *equilibrium* of the MAS.

One may then ask what happens if we perturb this equilibrium by introducing or removing certain amounts of one or more species. Such a perturbation generally alters the exact cancellation of forward and backward fluxes, typically driving the system away from detailed balance. For a reaction $r = y \to y'$, let $\nu_{r,s} := y'_s - y_s$ denote the *net stoichiometric coefficient* of s in r. Then the system and new concentrations c will still satisfy the *steady-state* condition for each species:

$$\frac{dc_s}{dt} = \sum_{r \in \overrightarrow{\mathcal{R}}} \nu_{r,s} J_r(c) = \eta_s, \quad \text{for all species } s \in \mathcal{S}. \tag{7}$$

Here $\eta_s \in \mathbb{R}$ denotes the net *external injection/removal rate* of species s. By convention, $\eta_s > 0$ means species s is injected from an external source, while $\eta_s < 0$ indicates a net removal of s. Note that (7) is invariant under the choice of direction in $\overrightarrow{\mathcal{R}}$, since

$$\nu_{r,s} J_r(c) = - - \nu_{\overline{r},s} J_{\overline{r}}(c).$$

We now introduce *chemical potentials* $\{\mu_s(c)\}_{s \in \mathcal{S}}$. For an MAS action system, these are defined as

$$\mu_s(c) := RT \ln(c_s) + \mu^0_s, \tag{8}$$

where R and T are the gas constant and absolute temperature, respectively. We can ignore the reference potential μ^0_s, since we are only interested in what happens to $\mu_s(c)$ under a

change of concentration $\delta c_s := c_s - c_s^*$. Applying the first-order Taylor expansion to $\ln(c_s)$ around c_s^* gives

$$\delta \ln(c_s) = \ln(c_s^* + \delta c_s) - \ln(c_s^*) \approx \frac{\delta c_s}{c_s^*},$$

so that

$$\delta \mu_s(c) = RT \delta \ln(c_s) \approx RT \frac{\delta c_s}{c_s^*}. \tag{9}$$

It is standard in linear non-equilibrium thermodynamics (see e.g. Chapter X in [53]) to assume (9) to be an equality, which is exact in the limit $\delta c_s / c_s^* \to 0$. We can apply the same first–order expansion to $J_r(c)$ (and assume equality), with $r = y \to y'$, obtaining

$$\delta J_r(c) = \sum_{s \in \mathcal{S}} \left. \frac{\partial J_r(c)}{\partial c_s} \right|_{c^*} \delta c_s = \sum_{s \in \mathcal{S}} \left(\frac{y_s}{c_s^*} \mathcal{K}_r(c^*) - \frac{y'_s}{c_s^*} \mathcal{K}_{\overline{r}}(c^*) \right) \delta c_s = -\mathcal{K}_r(c^*) \sum_{s \in \mathcal{S}} \frac{\nu_{r,s}}{c_s^*} \delta c_s. \tag{10}$$

By introducing the *affinity* of the reaction r

$$\Delta \mu_r(c) := -\sum_{s \in \mathcal{S}} \nu_{r,s} \delta \mu_s(c),$$

and the *Onsager coefficient*

$$G_r := \frac{\mathcal{K}_r(c^*)}{RT} > 0,$$

we have by (10) and (6) that

$$J_r(c) = J_r(c^*) + \delta J_r = G_r \Delta \mu_r(c) \tag{11}$$

The last thermodynamic quantity we need is the *instantaneous rate of Gibbs free–energy consumption* Φ:

$$\Phi(c) = \sum_{r \in \overrightarrow{\mathcal{R}}} J_r(c) \Delta \mu_r(c),$$

which measures the free–energy dissipated, i.e. the chemical "power" irreversibly lost (or supplied) by the running reactions, per unit time. Near equilibrium, we have due to (11) that

$$\Phi(c) = \sum_{r \in \overrightarrow{\mathcal{R}}} J_r(c)^2 / G_r. \tag{12}$$

Due to the square, we find that $\Phi(c)$ is invariant under the choice of direction in $\overrightarrow{\mathcal{R}}$, since $G_r = G_{\overline{r}}$.

D. Quantum walks

In this work we employ the use of quantum walk algorithms to compute properties of our chemical reaction network. Quantum walk algorithms provide a fundamentally different model of computation that is particularly well-suited for analysing graph-structured systems. In contrast to classical random walks, which explore a graph diffusively, quantum walks exhibit interference and coherence, allowing in some cases for more efficient exploration. For example, quantum walks offer quadratic speed-ups in search tasks [54–57] and, in some cases, even exponential improvements for structured graph problems [58]. These features suggest that quantum algorithms could help overcome the combinatorial complexity inherent in CRNs, where the number of pathways, intermediates, and reaction configurations grows rapidly with the system size.

We adopt the electric network framework introduced by [43] and further refined by [44, 59] to construct our quantum walks. These algorithms can likewise be derived via the span program formalism [60, 61].

While we primarily treat this framework as a black box to produce quantum walk algorithms with specified problem-solving capabilities and complexities, we also offer a brief overview of the principles underlying these quantum walks. Readers already familiar with the framework, or less interested in these details, may skip directly to the next section.

A quantum walk algorithm derived from the electrical network framework can be viewed as a specialised phase estimation algorithm [62]. Such an algorithm can be specified by the following parameters:

- A finite-dimensional complex inner product space H,
- a unit vector $|\psi_0\rangle \in H$,
- two subspaces $\mathcal{A}, \mathcal{B}$ of H, such that $|\psi_0\rangle \in \mathcal{B}^\perp$.

These parameters define a quantum algorithm as follows. Let

$$U_{\mathcal{AB}} = (2\Pi_{\mathcal{A}} - I)(2\Pi_{\mathcal{B}} - I). \tag{13}$$

We then perform phase estimation of $U_{\mathcal{AB}}$ on initial state $|\psi_0\rangle$ to a certain precision, measure the phase register, and output 1 if the measured phase is 0, and output 0 otherwise. Here

'perform phase estimation', means running a quantum subroutine that decides whether $|\psi_0\rangle$ has non-zero overlap with the $(+1)$-eigenspace of $U_{\mathcal{AB}}$, which, due to the structure of $U_{\mathcal{AB}}$, is precisely $(\mathcal{A}\cap\mathcal{B})\oplus(\mathcal{A}+\mathcal{B})^{\perp}$. Since by construction $|\psi_0\rangle$ is orthogonal to $\mathcal{B}$, the algorithm effectively decides whether $|\psi_0\rangle \in \mathcal{A}+\mathcal{B}$ or not.

The exact initialisation of the phase estimation parameters depends on the application, but in all our applications these parameters relate to objects from the classical random walk on the underlying graph and the electrical properties of the graph as an electrical network. For simplicity, we consider the simplest initialisation here, where $\mathrm{supp}(\sigma) = s$. The marked set M is either empty or equal to $\{t\}$ and it is the goal of the quantum walk to decide which case is true (assuming t is reachable from s).

The phase estimation algorithm takes place on the *edge space* of our network G:

$$\mathcal{H} = \mathrm{span}\{|u,v\rangle : \{u,v\} \in E(G)\}. \tag{14}$$

Note that each edge $\{u,v\} \in E(G)$ "appears twice" in $\mathcal{H}$: both as $|u,v\rangle$ and $|v,u\rangle$, which are orthogonal states in $\mathcal{H}$. This also means that intuitively our quantum walk will "walk on edges", where as a classical random walk on a graph usually takes place on its vertices.

The space $\mathcal{A}$ is constructed from the span of *star states*. For each vertex $u \in V(G)$, we define the normalised star state of $u \in V(G)$ as

$$|\psi_\star(u)\rangle := \frac{1}{\sqrt{\mathsf{w}_u}} \sum_{v\in\Gamma(u)} \sqrt{\mathsf{w}_{u,v}}|u,v\rangle, \tag{15}$$

where $\mathsf{w}_u := \sum_{v\in\Gamma(u)} \mathsf{w}_{u,v}$ is the *weighted degree* of u. This state can be seen as the quantum generalisation of the classical walk transition matrix: by measuring $|\psi_\star(u)\rangle$ we obtain the edge $|u,v\rangle$ with probability $\frac{\mathsf{w}_{u,v}}{\mathsf{w}_u}$. These star states are used to construct

$$\mathcal{A} = \mathrm{span}\{|\psi_\star(u)\rangle : u \in V \setminus \{s,t\}\}. \tag{16}$$

The other subspace $\mathcal{B}$ is the *antisymmetric subspace* of $\mathcal{H}$:

$$\mathcal{B} = \mathrm{span}\{|u,v\rangle + |v,u\rangle : (u,v) \in E(G)\}. \tag{17}$$

The last parameter $|\psi_0\rangle$ is the star state of s, projected onto the symmetric subspace of $\mathcal{H}$ to ensure orthogonality with $\mathcal{B}$:

$$|\psi_0\rangle = \sqrt{2}(I - \Pi_{\mathcal{B}})|\psi_\star(s)\rangle. \tag{18}$$

Since by assumption s and t are connected, we know that the s-t electrical flow θ exists and we can construct its corresponding (normalised) *flow state*, which is a quantum representation of the flow living in $\mathcal{B}^\perp$ (see (17)):

$$|\theta\rangle := \frac{1}{\sqrt{2\mathsf{E}(\theta)}} \sum_{(u,v)\in\vec{E}(G)} \frac{\theta_{u,v}}{\sqrt{\mathsf{w}_{u,v}}} \left(|u,v\rangle + |v,u\rangle\right). \tag{19}$$

The key observation in [43] is that, if $M = \{t\}$, the flow $|\theta\rangle$ lies in $(\mathcal{A}+\mathcal{B})^\perp$ and has non-zero overlap with $|\psi_0\rangle$, meaning that if s and t are connected, $|\psi_0\rangle \notin \mathcal{A}+\mathcal{B}$. Conversely, if $M = \emptyset$, it is shown that $|\psi_0\rangle \in \mathcal{A}+\mathcal{B}$.

E. The quantum walk algorithms

Depending on the application, we employ one of four quantum walk algorithms, discussed in this section. Their complexities depend on the required precision of the phase estimation, the cost of generating $|\psi_0\rangle$, and the cost of applying $U_{\mathcal{AB}}$. Since the initialisation of $|\psi_0\rangle$ and reflecting around spaces $\mathcal{A}, \mathcal{B}$ differs depending on the chosen algorithm, we express their complexities using abstract complexity parameters. For a graph G, marked set $M \subset V$ and distribution σ we define

- S: an upper bound on the cost of preparing the quantum state

$$|\sigma\rangle = \sum_{u\in\mathrm{supp}(\sigma)} \sigma(u)|u\rangle. \tag{20}$$

  This parameter captures the complexity of generating the initial state $|\psi_0\rangle$ (for further details, see Section 3.2.8 in [45]).

- $\mathsf{U}_\star$: an upper bound on the cost of verifying whether a vertex u belongs to $\mathrm{supp}(\sigma)$, the marked set M, or neither, as well as the cost of generating the star state $|\psi_\star(u)\rangle$ (see (15)) for any $u \in V \setminus (\{s\} \cup M)$. This parameter captures the complexity of implementing the quantum walk operator $U_{\mathcal{AB}}$ (for further details, see Section 3.2.5 in [45]).

The first algorithm we mention detects whether the marked set M is non-empty:

Theorem II.9 ([43]). *Fix a network $G = (V, E, \mathsf{w})$ as in Definition II.1, a marked set $M \subset V$ and an initial probability distribution σ on $V \setminus M$, with the promise that either*

M is empty or there is a path in G connecting σ to M. Then there exists a quantum walk algorithm that decides whether M is empty with a constant probability of success in cost

$$O(\mathsf{S} + \sqrt{\mathsf{R}_{\sigma,M}\mathsf{W}}\mathsf{U}_\star).$$

The above quantum walk is the only algorithm that we discuss in this work that is "purely" a phase estimation algorithm. All following algorithms combine (a slightly differently initialised) phase estimation routine with other well-known quantum subroutines. For more details, we refer the interested reader to their respective sources, as this is outside the scope of this work.

Our second algorithm does not detect, but actually returns these marked vertices.

Theorem II.10 ([59])**.** *Fix a network $G = (V, E, \mathsf{w})$ as in Definition II.1, a non-empty marked set $M \subset V$ and an initial probability distribution σ on $V \setminus M$, with the promise that there is a path in G connecting σ to M. Then there exists a quantum walk algorithm that returns a marked element from M with a constant probability of success in cost*

$$O(\mathsf{S} + \sqrt{\mathsf{R}_{\sigma,M}\mathsf{W}}\log^3(|M|)\mathsf{U}_\star).$$

The next two algorithms consider the special case where σ is supported on a single vertex and return information about the electrical network. They are parametrised with a quantity from [44] called *the escape time* $\mathsf{ET}_{s,M}$:

$$\mathsf{ET}_{s,M} := \frac{1}{\mathsf{R}_{s,M}} \sum_{u \in V(G)} \mathsf{p}_u^2 \mathsf{w}_u. \tag{21}$$

The operational meaning of this quantity is that it captures the expected time in which a random walk leaves s for the final time, before arriving in M. Since we know from electric network theory (specifically due to the fact that the effective resistance forms a metric) that $\mathsf{p}_u \leq p_s = \mathsf{R}_{s,M}$ for any vertex $u \in V$, the escape time $\mathsf{ET}_{s,M}$ lower bounds $\mathsf{R}_{s,M}\mathsf{W}$.

Our third and fourth algorithm are based on the *alternative neighbourhood* technique from [45], which we shall discuss in Section IV, and they generalise the following two quantum algorithms. The first algorithm approximates the effective resistance $\mathsf{R}_{s,M}$ (up to the weighted degree w_s of s).

Theorem II.11 ([44])**.** *Fix a network $G = (V, E, \mathsf{w})$ as in Definition II.1, a non-empty marked set $M \subset V$ and an initial vertex $s \in V \setminus M$, with the promise that there is a path*

in G connecting s to M. Then there exists a quantum walk algorithm that ϵ-multiplicatively estimates $\mathsf{R}_{s,M}\mathsf{w}_s$ with a constant probability of success in cost

$$O\left(\frac{1}{\epsilon}\left(\mathsf{S}+\frac{1}{\epsilon}\left(\mathsf{ET}_{s,M}+\log(\mathsf{R}_{s,M}\mathsf{w}_s)\right)\mathsf{U}_\star\right)\right).$$

The second algorithm generates an approximation of the flow state corresponding to the s-M electrical flow θ:

Theorem II.12 ([44, 61])**.** *Fix a network $G=(V,E,\mathsf{w})$ as in Definition II.1, a non-empty marked set $M\subset V$ and an initial vertex $s\in V\setminus M$, with the promise that there is a path in G connecting s to M. Let θ be the s-M electrical flow on G with corresponding flow state $|\theta\rangle$ as defined in (19). Then there exists a quantum walk algorithm that returns a state $|\widetilde{\theta}\rangle$ satisfying*

$$\frac{1}{2}\left\||\widetilde{\theta}\rangle\langle\widetilde{\theta}|-|\theta\rangle\langle\theta|\right\|\leq\epsilon$$

with a constant probability of success in cost

$$O\left(\mathsf{S}+\frac{1}{\epsilon^2}\left(\sqrt{\mathsf{ET}_{s,M}}+\log(\mathsf{R}_{s,M}\mathsf{w}_s)\right)\mathsf{U}_\star\right).$$

Note that to successfully run the above quantum algorithms, we need to know the precision with which to run the phase estimation subroutine, for which we need to know upper bounds on $\mathsf{R}_{s,M}$, w_s, W and $\mathsf{ET}_{s,M}$ before running the algorithm. If these quantities are not known beforehand, the algorithms (and their corresponding complexities) can also be instantiated with (trivial) upper bounds on these quantities.

III. REPRESENTING AN MAS AS AN ELECTRICAL NETWORK

A. The mass action system graph

In this work, we represent an MAS as an electrical network, to allow us to run a quantum walk algorithm on this network. To create this electrical network, we base our approach on the bipartite graph representation by [63]. In this bipartite graph representation, the set of species, $\mathcal{S}$, forms one partition of the vertices and the set of reactions, $\mathcal{R}$, forms the other. A directed edge, or *arc*, is drawn between a species $s\in\mathcal{S}$ and a reaction $y\to y'\in\mathcal{R}$ if and only if species s occurs with non-zero stoichiometry in the reactant complex y, that is, $y_s\neq 0$. Similarly, an arc is drawn between a reaction $y\to y'\in\mathcal{R}$ and a species $s\in\mathcal{S}$

when s occurs with non-zero stoichiometry in the product complex y'. Note that although the formal definition of a chemical reaction network (CRN) includes the set of complexes $\mathcal{C}$, this representation does not. In many analyses, including our graph-based approach, the essential information provided by the complexes is fully encoded within the reactions themselves. Each reaction inherently describes the transformation from a set of reactant species to a set of product species. Therefore, by representing the CRN as a bipartite graph with one partition corresponding to the species $\mathcal{S}$ and the other to the reactions $\mathcal{R}$, we retain all critical stoichiometric information. Unlike other graph representations of CRNs, this bipartite graph ensures that each reactant is represented only once while remaining correctly connected to its associated reactions.

To represent an MAS as an electrical network, we are not allowed to have any directed edges (see Definition II.1), meaning that this approach will not suffice. In addition, the thermodynamic machinery discussed in Section II C also needs our MAS to have additional structure. We will therefore assume in the rest of this work that our MAS $(\mathcal{S}, \mathcal{C}, \mathcal{R}, k)$ satisfies the following three conditions:

1. The underlying CRN of our MAS is **reversible** (every reaction $y \to y'$ appears together with its backward reaction $y' \to y$ in $\mathcal{R}$), meaning we can fully characterise $\mathcal{R}$ by the set of oriented reactions $\overrightarrow{\mathcal{R}}$.

2. The MAS admits a positive equilibrium concentrations vector c^* that realises **detailed balance**, i.e. the forward and reverse fluxes of every reaction pair coincide at c^*.

3. Each reaction in $\mathcal{R}$ is **particle conserving**, meaning that for every $y \to y' \in \mathcal{R}$ we have $\sum_s y_s = \sum_s y'_s$.

In practice, many mechanistic models violate at least one of these assumptions: combustion schemes contain intrinsically irreversible steps, metabolic networks include "committed" reactions, and numerous biological or catalytic processes are deliberately driven far from equilibrium, so that neither a detailed-balance concentration nor particle conservation holds exactly. Nevertheless, imposing these constraint is a standard assumption to simplify the analysis of chemical kinetics within the CRN framework. Additionally, we shall shortly see that under these assumption, the dynamical properties of our MAS will give rise to a duality with electrical networks.

Under the assumptions of reversibility, detailed balance, and particle conserving, our bipartite graph representation is formally defined as follows:

Definition III.1 (Mass Action System Graph)**.** *For an MAS $(\mathcal{S}, \mathcal{C}, \mathcal{R}, k)$ and a concentrations vector $c \in \mathbb{R}^{\mathcal{S}}_{\geq 0}$ its mass action system graph (MASG) is a weighted bipartite undirected graph $G = (V, \overline{E}, \mathsf{w})$, where:*

- *The vertex set V is the disjoint union of species and (reversible) reactions, given by $V = \mathcal{S} \sqcup \overrightarrow{\mathcal{R}}$, where $\mathcal{S}$ is the set of species and $\overrightarrow{\mathcal{R}}$ is the set of oriented reactions.*
- *The edge set $E \subseteq \{\{s, r\} \mid s \in \mathcal{S}, r \in \overrightarrow{\mathcal{R}}\}$ consists of edges connecting species to reactions. An edge $\{s, r\}$ is part of E if and only if s appears with non-zero stoichiometry in r, i.e. at least one of y_s, y'_s is non zero for $r = y \to y'$. The directed edge set $\overrightarrow{E}$ is obtained by considering the direction (s, r) for every $\{s, r\} \in E$.*
- *The weight function $\mathsf{w} : E \to \mathbb{R}_{>0}$ is defined on the edge set E, where each edge $\{s, r\}$ is weighted by $\nu_r \, |\nu_{r,s}| \, G_r$, where $\nu_r := \sum_{s \in \mathcal{S}} |\nu_{r,s}|$.*

Note that G is invariant under the choice of direction in $\overrightarrow{\mathcal{R}}$, since $\nu_r = \nu_{\overline{r}}$. To obtain some intuition for the construction of MASG in Definition III.1, we return to our example from (2). We make some small modifications to the CRN to ensure that it is reversible and particle conserving. For readability, we also relabel the reactions as follows:

$$\begin{aligned} A &\underset{r_2}{\overset{r_1}{\rightleftharpoons}} B, \\ A + C &\underset{r_4}{\overset{r_3}{\rightleftharpoons}} 2D, \\ D + 2B &\underset{r_6}{\overset{r_5}{\rightleftharpoons}} 3E. \end{aligned} \tag{22}$$

The resulting MASG is shown in Figure 2.

B. The flow on an MASG

For an MAS $(\mathcal{S}, \mathcal{C}, \mathcal{R}, k)$, consider a marked set of species $M \subseteq \mathcal{S}$ and a probability distribution σ on $\mathcal{S} \setminus M$. Let $c_{\sigma,M} \in \mathbb{R}^{\mathcal{S}}_{\geq 0}$ be the concentrations vector obtained by slightly perturbing the equilibrium c^* through the addition of species, characterised by η (see (7)), such that

$$\eta_s = \sigma(s), \qquad \sum_{s \in M} \eta_s = -1. \tag{23}$$

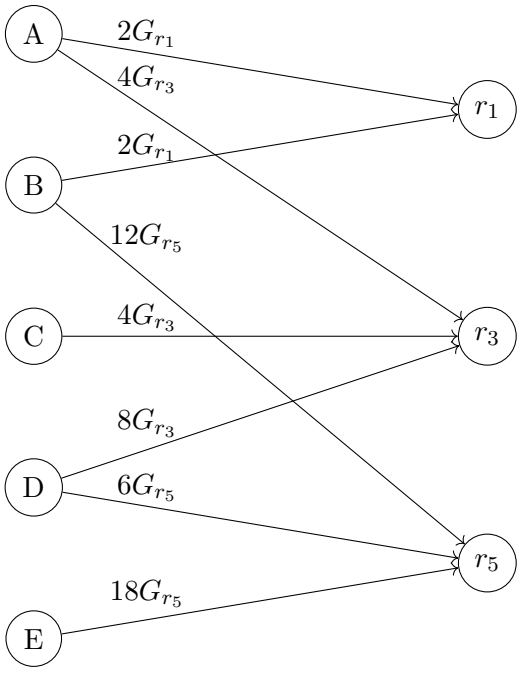

Figure 2. The resulting MASG for the CRN in (22).

We exhibit a σ-M flow θ on the MASG obtained from the MAS $(\mathcal{S}, \mathcal{C}, \mathcal{R}, k)$ and concentrations vector $c_{\sigma,M}$. This flow θ will hence have to satisfy Kirchoff's Law (see Definition II.5), but it does not necessarily coincide with the actual σ-M electrical flow on the MASG, meaning it does not need to satisfy Ohm's Law (see Definition II.6).

Lemma III.2. *For an MASG $G = (V, E, \mathsf{w})$ obtained from an MAS $(\mathcal{S}, \mathcal{C}, \mathcal{R}, k)$ and a concentrations vector $c \in \mathbb{R}^{\mathcal{S}}_{\geq 0}$, the following assignment of flow θ to the edges $\overrightarrow{E}$ is a valid unit σ-M flow on G:*

$$\theta_{s,r} = \nu_{r,s} J_r(c_{\sigma,M}), \tag{24}$$

where $J_r(c_{\sigma,M})$ is the net flux of the reaction r under the concentrations vector $c_{\sigma,M}$ (see (5)).

Proof. To show that θ is a unit σ-M flow on G, we must show that it satisfies Kirchhoff's Law, as well as that $\theta_s = \sigma(s)$ for every s in the support of σ and $\sum_{s \in M} \theta_s = -1$.

We split Kirchhoff's Law into two parts tackling the vertices in $\mathcal{S}$ and $\overrightarrow{\mathcal{R}}$ separately. Starting with $\overrightarrow{\mathcal{R}}$, we know by assumption that our MAS is particle conserving. Hence for every $r = y \to y' \in \overrightarrow{\mathcal{R}}$, we have

$$\sum_{s \in \mathcal{S}} \theta_{r,s} = -J_r(c_{\sigma,M}) \sum_{s \in \mathcal{S}} \nu_{r,s} = -J_r(c_{\sigma,M}) \sum_{s \in \mathcal{S}} (y'_s - y_s) = 0.$$

We combine Kirchhoff's Law for the vertices in $\mathcal{S}$ with the other requirements, namely $\theta_s = \sigma(s)$ for every s in the support of σ and $\sum_{s\in M} \theta_s = -1$, since all of these follow from the fact that $c_{\sigma,M}$ satisfies the steady-state condition (see (7)), meaning that for every $s \in \mathcal{S}$ we have:

$$\sum_{r\in\overrightarrow{\mathcal{R}}} \theta_{r,s} = \sum_{r\in\overrightarrow{\mathcal{R}}} \nu_{r,s} J_r(c_{\sigma,M}) = \eta_s.$$

By (23), we know that $\eta_s = \sigma(s)$ for every $s \in \mathcal{S} \setminus M$ and that $\sum_{s\in M} \eta_s = -1$, which completes the proof. □

We will refer to the flow from (24) as the MASG flow. Now that we know that the MASG flow is a unit σ-M flow by Lemma III.2, we can calculate its energy $\mathsf{E}(\theta)$:

$$\mathsf{E}(\theta) = \sum_{s\in\mathcal{S}} \sum_{r\in\overrightarrow{\mathcal{R}}} \frac{\theta_{s,r}^2}{\mathsf{w}_{s,r}} = \sum_{s\in\mathcal{S}} \sum_{r\in\overrightarrow{\mathcal{R}}} \frac{\nu_{r,s}^2 J_r(c_{\sigma,M})^2}{\nu_r \left|\nu_{r,s}\right| G_r} = \sum_{r\in\overrightarrow{\mathcal{R}}} \frac{J_r(c_{\sigma,M})^2}{G_r}. \tag{25}$$

Note that this precisely matches the instantaneous rate of Gibbs free–energy consumption $\Phi(c_{\sigma,M})$ from (12).

In this section, we have shown an MASG can be represented as an electrical network, such that its dynamics map directly to those of the electrical network, and hence to the quantum-walk parameters. Table I summarises this connection.

C. The computational cost

Using our electrical network representation of the MAS, we develop quantum walk algorithms to answer structural and kinetic questions about the underlying chemical reaction network. These constructions apply to MASs that are particle-conserving, reversible, and admit a detailed balance condition.

The asymptotic cost of these algorithms relies on the abstract costs from Section II E: S, i.e. setting up the state $|\sigma\rangle$, and $U_\star$, i.e. the cost of implementing the quantum walk operator $U_{\mathcal{AB}}$ from (13), or equivalently, the cost of implementing the star states $|\psi_\star(u)\rangle$.

MASG	Electrical network
Species $\mathcal{S}$	Vertices $\mathcal{S}$ forming an independent set
Oriented reactions $\overrightarrow{\mathcal{R}}$	Vertices $\overrightarrow{\mathcal{R}}$ forming an independent set
Target species in $\mathcal{S}$	Marked set $M \subseteq \mathcal{S}$
External injection/removal rate η_s	Initial probability distribution $\sigma(s)$
Non-zero stoichiometric coefficient of $s \in \mathcal{S}$ in $r \in \overrightarrow{\mathcal{R}}$	Directed edge (s, r)
Thermodynamical quantity $\nu_r \lvert\nu_{r,s}\rvert G_r$	Edge conductance $\mathsf{w}_{s,r}$
Thermodynamical quantity $\nu_{r,s} J_r(c_{\sigma,M})$	Valid unit s-M flow $\theta_{s,r}$
Gibbs free-energy consumption $\Phi(c_{\sigma,M})$	Energy $\mathsf{E}(\theta)$ of the MASG flow

Table I. A summary of how our MASG representation connects the CRN and its dynamics to an electrical network.

The states relevant to these costs are therefore

$$\begin{aligned} |\sigma\rangle &= \sum_{s\in\mathcal{S}\setminus M} \sqrt{\eta_s}|s\rangle, \\ |\psi_\star(s)\rangle &= \frac{1}{\sqrt{\sum_{r\in\overrightarrow{\mathcal{R}}} \nu_r \lvert\nu_{r,s}\rvert G_r}} \sum_{r\in\overrightarrow{\mathcal{R}}} \sqrt{\nu_r \lvert\nu_{r,s}\rvert G_r}|s, r\rangle, \\ |\psi_\star(r)\rangle &= \frac{1}{\sqrt{\nu_r}} \sum_{s\in\mathcal{S}} \sqrt{\nu_{r,s}}|r, s\rangle. \end{aligned} \tag{26}$$

For typical applications of our framework it is reasonable to assume that these quantum states can be prepared efficiently. Because we focus on near-equilibrium dynamics (see Section II C), we assume that the MAS is initially close to a known steady state c^* and that all thermodynamic quantities required with respect to this equilibrium can be pre-computed classically. Storing these values in read-only QRAM then allows efficient generation of the states in (26).

D. Detecting and finding reachable species

We are now ready to describe our quantum algorithms for deciding whether a given set of target species is reachable, and for outputting a target species if this is the case.

Corollary III.3. *Fix an MAS $(\mathcal{S}, \mathcal{C}, \mathcal{R}, k)$ that admits a detailed balance, that is particle conserving and whose underlying CRN is reversible. Fix an initial distribution of species σ on $\mathcal{S}$ and a set of target species M, and let S be the cost of generating the state $|\sigma\rangle$. Then there exists a quantum walk algorithm that decides whether any of the target species in M is reachable from σ with a constant probability of success in cost*

$$\mathsf{S} + \sqrt{\Phi(c_{\sigma,M}) \sum_{r \in \overrightarrow{\mathcal{R}}} \nu_r^2 G_r}.$$

Proof. We invoke Theorem II.9 to obtain a quantum walk that runs on the MASG obtained from our MAS. By our choice of weights for the MASG, we know that

$$\mathsf{W} = \sum_{r \in \overrightarrow{\mathcal{R}}} \sum_{s \in \mathcal{S}} \nu_r \left|\nu_{r,s}\right| G_r = \sum_{r \in \overrightarrow{\mathcal{R}}} \nu_r^2 G_r.$$

Lastly, we know by (25) that the energy of the MASG flow allows us to upper bound the effective resistance as follows:

$$\mathsf{R}_{\sigma,M} \leq \mathsf{E}(\theta) = \Phi(c_{\sigma,M}). \qquad \square$$

Corollary III.4. *Fix an MAS $(\mathcal{S}, \mathcal{C}, \mathcal{R}, k)$ that admits a detailed balance, that is particle conserving and whose underlying CRN is reversible. Fix an initial distribution of species σ on $\mathcal{S}$ and a non-empty set of target species M, reachable from σ. Then there exists a quantum walk algorithm that returns any of the target species from M with a constant probability of success in cost*

$$\mathsf{S} + \sqrt{\Phi(c_{\sigma,M}) \sum_{r \in \overrightarrow{\mathcal{R}}} \nu_r^2 G_r} \log^3(|M|).$$

Proof. This follows directly from Theorem II.10, by applying the same parameters as in Corollary III.3. $\square$

IV. ALGORITHMS FOR THE GIBBS FREE-ENERGY CONSUMPTION

At a first glance, one might hope to approximate the Gibbs free energy consumption $\Phi(c_{s,M})$ using Theorem II.11, since (25) guarantees that for the MASG flow we have

$$\mathsf{R}_{s,M} \leq \mathsf{E}(\theta) = \Phi(c_{s,M}).$$

However, the flow θ constructed in (25) does not, in general, coincide with the true σ-M electrical flow. As a result, we typically have $\mathsf{R}_{s,M} < \Phi(c_{s,M})$. Consequently, applying Theorem II.11 yields only an approximation to a lower bound on $\Phi(c_{s,M})$, and the tightness of this bound is unclear. In this section, we show how we resolve this problem in certain cases.

A. Multidimensional electrical networks

Ref. [45] introduces the multidimensional quantum walk framework to generalise the standard quantum walk framework, later further formalised in [46]. A key innovation in this generalisation is the introduction of *alternative neighbourhoods*.

Definition IV.1 (Alternative Neighbourhoods)**.** *For a network $G = (V, E, \mathsf{w})$, as in Definition II.1, a set of* alternative neighbourhoods *is a collection of states:*

$$\Psi_\star = \{\Psi_\star(u) \subset \operatorname{span}\{|u, v\rangle : |u, v\rangle : v \in \Gamma(u)\} : u \in V\}$$

such that for all $u \in V$, $|\psi_\star(u)\rangle \in \Psi_\star(u)$ (see (15)). We view the states of $\Psi_\star(u)$ as different possibilities for $|\psi_\star(u)\rangle$, only one of which is "correct".

By adding additional alternative neighbourhoods to the set $\Psi_{\mathcal{A}}$ spanning $\mathcal{A}$ (see (16)), we obtain $\Psi_{\mathcal{A}^{\mathsf{alt}}}$. In the rest of this section, we assume that each $\Psi(u)$ is a normalised basis $\{|\psi_{u,0}\rangle = |\psi_\star(u)\rangle, \ldots, |\psi_{u,a_u-1}\rangle\}$, so

$$\Psi_{\mathcal{A}^{\mathsf{alt}}} = \{|\psi_{u,i}\rangle : u \in V \setminus (\{s\} \cup M), i \in \{0, \ldots, a_u - 1\}.$$

Through the addition of these alternative neighbourhoods, we obtain the modified quantum walk operator

$$U_{\mathcal{A}^{\mathsf{alt}}\mathcal{B}} = (2\Pi_{\mathcal{A}^{\mathsf{alt}}} - I)(2\Pi_{\mathcal{B}} - I), \tag{27}$$

Here, $\Pi_{\mathcal{A}^{\mathsf{alt}}}$ denotes the orthogonal projector onto the modified star space $\mathcal{A}^{\mathsf{alt}}$.

Incorporating these additional neighbourhoods into $\Psi_\star(u)$ alters the quantum walk operator, and thus the complexity of its implementation. This was central to their original introduction in [45], as these constructions are necessary in applications where it is computationally much more efficient to generate the set $\Psi_\star(u)$ rather than the individual star state $|\psi_\star(u)\rangle$. For example, this situation arises when $|\psi_\star(u)\rangle$ is known to be one of a small collection of easily preparable states within $\Psi_\star(u)$, but it is computationally infeasible to determine precisely which one. We denote the cost of implementing $U_{\mathcal{A}^{\mathsf{alt}}\mathcal{B}}$ by $\mathsf{U}_\star^{\mathsf{alt}}$.

It was later shown in [47], that the addition of alternative neighbourhoods structure in this way gives rise to the σ-M alternative electrical flow associated with $\Psi_\star$. This flow satisfies the *Alternative Kirchhoff's Law* and *Alternative Ohm's Law*, which generalise Definition II.5 and Definition II.6, respectively.

Definition IV.2 (Kirchhoff's Alternative Law)**.** *For any s-M alternative flow θ^{alt} with respect to a collection of alternative neighbourhoods $\Psi_\star$ on an electrical network $G = (V, E, \mathsf{w})$, the corresponding flow state $|\theta^{\mathsf{alt}}\rangle$ is orthogonal to* $\mathrm{span}(\Psi_\star(u))$ *for every $u \in V \backslash \{\{s\} \cup M\}$, that is, $\langle \psi_{u,i} | \theta \rangle = 0$ for each $i \in \{0, 1, \cdots, a_u - 1\}$.*

Definition IV.3 (Alternative Electrical Flow)**.** *For a collection of alternative neighbourhoods $\Psi_\star$ on an electrical network $G = (V, E, \mathsf{w})$, the s-M* alternative electrical flow *is the unique alternative unit s-M flow θ^{alt} with minimal energy $\mathsf{E}(\theta^{\mathsf{alt}})$. We call this minimal energy the* alternative effective resistance $\mathsf{R}^{\mathsf{alt}}_{s,t}$.

Definition IV.4 (Alternative Ohm's Law)**.** *Let θ^{alt} be the s-M alternative electrical flow with respect to a collection of alternative neighbourhoods $\Psi_\star$ on an electrical network $G = (V, E, \mathsf{w})$. Then there exists an alternative potential vector $\mathsf{p}^{\mathsf{alt}}$ corresponding to θ^{alt}, which assigns a unique potential $\mathsf{p}^{\mathsf{alt}}_{u,v}$ to each edge $(u, v) \in E$ such that $\mathsf{p}^{\mathsf{alt}}_{s,v} = \mathsf{R}^{\mathsf{alt}}_{s,t}$ for every $v \in \Gamma(s)$ and $\mathsf{p}^{\mathsf{alt}}_{u,v} = 0$ for every $u \in M$ and $v \in \Gamma(u)$. Additionally, the associated state $|\mathsf{p}^{\mathsf{alt}}\rangle$ (see (16) in [47]) satisfies $\Pi_{\mathcal{A}^{\mathsf{alt}}} |\mathsf{p}^{\mathsf{alt}}\rangle = |\mathsf{p}^{\mathsf{alt}}\rangle$ and the potential difference between (u, v) and (v, u) is equal to the amount of electrical flow $\theta^{\mathsf{alt}}_{u,v}$ along (u, v) multiplied with the resistance $1/\mathsf{w}_{u,v}$, that is, $\mathsf{p}^{\mathsf{alt}}_{u,v} - \mathsf{p}^{\mathsf{alt}}_{v,u} = \theta^{\mathsf{alt}}_{u,v}/\mathsf{w}_{u,v}$.*

The alternative potential $\mathsf{p}^{\mathsf{alt}}$ from Definition IV.4 gives rise to an alternative escape time,

generalising (21):

$$\mathsf{ET}^{\mathsf{alt}}_{s,M} := \frac{1}{\mathsf{R}^{\mathsf{alt}}_{s,M}} \sum_{u,v\in E} \mathsf{p}^2_{u,v}\mathsf{w}_{u,v}. \tag{28}$$

By using these "alternative" electrical network definitions, Ref. [47] shows that we can approximate the alternative electrical flow, generalising Theorem II.12 to alternative neighbourhoods:

Theorem IV.5 ([47]). *Fix a network $G = (V, E, \mathsf{w})$ as in Definition II.1, a collection of alternative neighbourhoods $\Psi_\star$, a non-empty marked set $M \subset V$ and an initial vertex $s \in V \setminus M$, with the promise that there is a path in G connecting s to M. Let θ^{alt} be the s-M alternative electrical flow on G with corresponding flow state $|\theta^{\mathsf{alt}}\rangle$ as defined in (19). Then there exists a quantum walk algorithm that returns a state $|\widetilde{\theta}\rangle$ satisfying*

$$\frac{1}{2}\left\||\widetilde{\theta}\rangle\langle\widetilde{\theta}| - |\theta^{\mathsf{alt}}\rangle\langle\theta^{\mathsf{alt}}|\right\| \leq \epsilon$$

with a constant probability of success in cost

$$O\left(\mathsf{S} + \frac{1}{\epsilon^2}\left(\sqrt{\mathsf{ET}^{\mathsf{alt}}_{s,M}} + \log(\mathsf{R}^{\mathsf{alt}}_{s,M}\mathsf{w}_s)\right)\mathsf{U}^{\mathsf{alt}}_\star\right).$$

B. Using alternative neighbourhoods to restrict the flow

The technique of alternative neighbourhoods has previously been employed in [45–47] to address the cases where it is computationally easier to generate $\Psi_\star(u)$, which includes additional alternative neighbourhoods, than to construct the star state $|\psi_\star(u)\rangle$ directly. In this section, we exhibit a novel use of this technique: we show how alternative neighbourhoods can be leveraged to approximate the Gibbs free-energy consumption, and to prepare a quantum state that is a superposition over all species-reaction pairs (r, s), weighted by their contribution to the total Gibbs free-energy consumption.

Our approach constructs a collection of alternative neighbourhoods $\Psi_\star$ such that the MASG flow defined in (24) is the unique s-M flow satisfying Alternative Kirchhoff's Law (see Definition IV.2). By construction (see Definition IV.3), this guarantees that the MASG flow is also the alternative s-M electrical flow with respect to $\Psi_\star$.

This reverses the usual causal relationship between alternative neighbourhoods and the corresponding electrical flow: rather than beginning with a prescribed set $\Psi_\star$ and checking

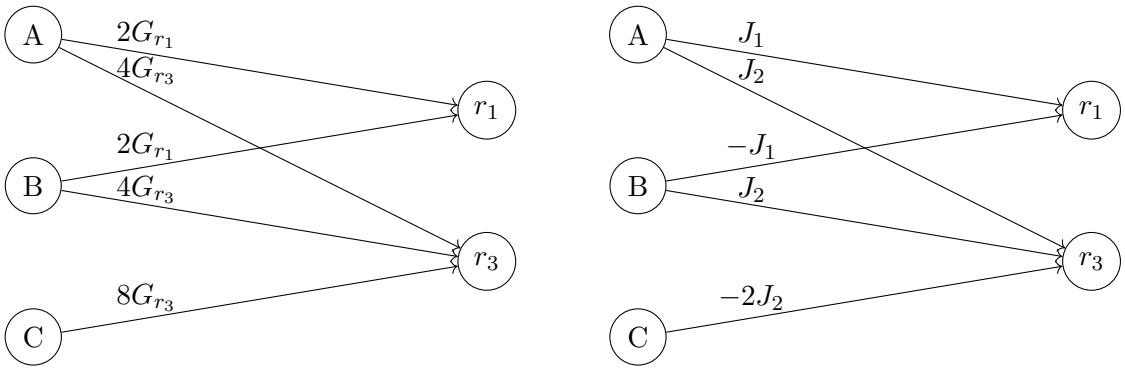

Figure 3. The resulting MASG for the CRN in (29). The left image shows the weight assignments of each (directed) edge, the right image shows the corresponding flow values for the MASG flow, where for notational clarity we have omitted the argument $(c_{s,M})$ for each net flux J_r.

which flows satisfy Alternative Kirchhoff's Law, we start from the desired flow and reverse-engineer the alternative neighbourhoods $\Psi_\star$ so that this flow becomes the alternative s-M electrical flow relative to $\Psi_\star$.

1. *An example*

To give an example of how this works, we consider the following simple CRN

$$\begin{aligned} A &\underset{r_2}{\overset{r_1}{\rightleftharpoons}} B, \\ A + B &\underset{r_4}{\overset{r_3}{\rightleftharpoons}} 2C. \end{aligned} \tag{29}$$

We let $\eta_A = -\eta_C = 1$ and show the resulting MASG and corresponding MASG flow (which is a unit flow from A to C) in Figure 3.

By Lemma III.2, we know that the MASG flow is a unit flow satisfying Kirchhoff's Law. In particular, this means that $J_1 = J_2 = \frac{1}{2}$. There is no guarantee that this flow matches A-C electrical flow on the MASG. In fact, for the simplified case where all $G_r = 1$, we see that the flow is not optimal, as shown in Figure 4.

Recall from (15) that the star state for the vertex r_3 is given by

$$\begin{aligned} |\psi_\star(r_3)\rangle &= \frac{1}{\sqrt{\mathsf{W}_{r_3}}} \left(\sum_{v \in \Gamma^+(r_3)} \sqrt{\mathsf{W}_{r_3,v}} |r_3, v\rangle - \sum_{v \in \Gamma^-(r_3)} \sqrt{\mathsf{W}_{r_3,v}} |r_3, v\rangle \right) \\ &= \frac{1}{2} \left(-|r_3, A\rangle - |r_3, B\rangle - \sqrt{2}|r_3, C\rangle \right). \end{aligned}$$

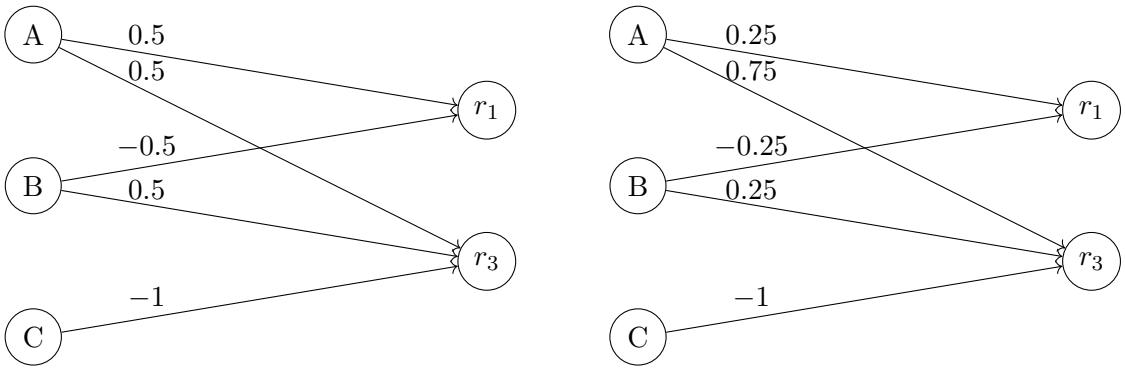

Figure 4. The MASG flow for $J_1 = J_2 = \frac{1}{2}$ is shown on the left and an A-C flow with lower energy (assuming all $G_r = 1$) is shown on the right, disproving the fact that our MASG flow matches the A-C electrical flow.

Now suppose that we add an alternative neighbourhood to $\Psi_\star(r_3)$:

$$\Psi_\star(r_3) = \left\{ \frac{1}{2}\left(-|r_3, A\rangle - |r_3, B\rangle - \sqrt{2}|r_3, C\rangle\right), \frac{1}{\sqrt{2}}\left(|r_3, A\rangle - |r_3, B\rangle\right) \right\}. \tag{30}$$

This means that $\Psi_\star(r_3)$ forms a basis for a 2-dimensional subspace of the 3-dimensional subspace spanned by the states $\{|r_3, A\rangle, |r_3, B\rangle, |r_3, C\rangle\}$. The flow state of any alternative A-C flow satisfying Alternative Kirchhoff's Law must be orthogonal to this subspace, meaning in particular that

$$\langle\theta|\frac{1}{2}\left(-|r_3, A\rangle - |r_3, B\rangle - \sqrt{2}|r_3, C\rangle\right) = -\frac{1}{2\sqrt{4G_{r_3}}}\left(\theta_{r_3,A} + \theta_{r_3,B} + \theta_{r_3,C}\right) = 0,$$

which is equivalent to the flow being conserved at r_3, and

$$\langle\theta|\frac{1}{\sqrt{2}}\left(|r_3, A\rangle - |r_3, B\rangle\right) = \frac{1}{2\sqrt{4G_{r_3}}}\left(\theta_{r_3,A} - \theta_{r_3,B}\right) = 0,$$

which forces $\theta_{r_3,A} = \theta_{r_3,B}$. Jointly, these constraints leave us only with a single option for the flow through r_3, since θ must also be a unit flow from A to C:

$$2\theta_{r_3,A} = 2\theta_{r_3,B} = -\theta_{r_3,C} = 1.$$

Note that this immediately fixes the rest of the flow as well, since the outgoing flow of A must be 1, recovering the MASG flow.

2. *The general case*

Contrary to how alternative neighbourhoods are usually applied, we start with our target MASG flow θ and reverse engineer our alternative neighbourhoods such that θ is precisely the alternative s-M electrical flow. We start with $r \in \overrightarrow{\mathcal{R}}$, where the normalised projection of $|\theta\rangle$ (where θ is our MASG flow) onto $\text{span}\{|r,s\rangle : s \in \mathcal{S}\}$ is equal to

$$|\theta_r\rangle := \frac{1}{\sqrt{\sum_{s\in\mathcal{S}} \nu_{r,s}^2}} \sum_{s\in\mathcal{S}} \nu_{r,s}|r,s\rangle. \tag{31}$$

As discussed in Section III C, it is reasonable to assume that this state can be prepared efficiently in practical settings: the ratios of stoichiometric coefficients for the species involved in each reaction can be pre-computed classically and stored in QRAM.

In principle, performing the same preparation for every $s \in \mathcal{S}\setminus M$ would always reproduce the MASG flow. Unfortunately, this is not computationally viable in general. For $s \in \mathcal{S}\setminus M$, the normalised projection of $|\theta\rangle$ onto $\text{span}\{|r,s\rangle : r \in \mathcal{R}\}$ is

$$|\theta_s\rangle := \frac{1}{\sqrt{\sum_{r\in\overrightarrow{\mathcal{R}}} \nu_{r,s}^2 J_r(c_{\sigma,M})^2}} \sum_{r\in\overrightarrow{\mathcal{R}}} \nu_{r,s} J_r(c_{\sigma,M})|r,s\rangle. \tag{32}$$

Preparing this state requires knowledge of the relative fluxes $J_r(c_{\sigma,M})$ for all $r \in \mathcal{R}$. These fluxes depend on the steady-state concentrations $c_{\sigma,M}$, which can be obtained only by solving a global system of polynomial equations for the entire MAS, a task that is computationally infeasible. Consequently, we cannot generate the state in (32) and must restrict our alternative neighbourhood construction to vertices in $\mathcal{R}$.

The example in Figure 4 shows that this restriction *can* be sufficient to recover the MASG flow uniquely, but it is not guaranteed for all networks. We therefore confine our attention to the following class of networks:

Definition IV.6 (σ-M Rigid Network)**.** *Let $G = (V, E, \mathsf{w})$ be a network as in Definition II.1, let $M \subset V$ be a non-empty marked set, and let σ be a probability distribution supported on $V \setminus M$. We say that G is s-M* rigid *if the following conditions hold:*

- *G is bipartite with vertex partition $V = V_A \sqcup V_B$,*
- *σ is supported entirely on V_A,*

- *For each $b \in V_B$, we fix a ratio vector $\rho_b : V_A \to \mathbb{R}_{\neq 0}$, supported on the neighbours of b,*

- *Under these conditions, there exists a* unique *s-M flow θ such that for all $b \in V_B$ and all $a_1, a_2 \in V_A$ such that $(b, a_1), (b, a_2) \in E$ and $\rho_b(a_1), \rho_b(a_2)$,*

$$\frac{\theta(b, a_1)}{\rho_b(a_1)} = \frac{\theta(b, a_2)}{\rho_b(a_2)}.$$

Provided the MASG is s-M rigid, we can apply our alternative neighbourhood technique to ensure that the MASG flow is the *unique* s-M flow satisfying Alternative Kirchhoff's Law.

C. Approximating and sampling from the Gibbs free-energy consumptions

Our quantum algorithm to estimate the Gibbs free-energy consumption is an extension of Theorem II.11 that accommodates the use of alternative neighbourhoods:

Theorem IV.7 ([44]). *Fix a network $G = (V, E, \mathsf{w})$ as in Definition II.1, a collection of alternative neighbourhoods $\Psi_\star$, a non-empty marked set $M \subset V$ and an initial vertex $s \in V \setminus M$, with the promise that there is a path in G connecting s to M. Then there exists a quantum walk algorithm that ϵ-multiplicatively estimates $\mathsf{R}^{\mathsf{alt}}_{s,M}$ with a constant probability of success in cost*

$$O\left(\frac{1}{\epsilon}\left(\mathsf{S} + \frac{1}{\epsilon}\left(\mathsf{ET}^{\mathsf{alt}}_{s,M} + \log(\mathsf{R}^{\mathsf{alt}}_{s,M}\mathsf{w}_s)\right)\mathsf{U}^{\mathsf{alt}}_\star\right)\right).$$

Proof. The proof combines the strategy of the proof of Theorem II.11 from [44], with Theorem 1.1 and Lemma 2.12 from [47]. These theorems state that if we apply phase estimation with precision $O(\epsilon/(\mathsf{ET}^{\mathsf{alt}}_{s,M}\mathsf{R}^{\mathsf{alt}}_{s,M}\mathsf{w}_s)$ to the modified quantum walk operator $U_{\mathcal{A}^{\mathsf{alt}}\mathcal{B}}$ from (27), the probability of the phase estimation register yielding "0" is $p' = (1 \pm \epsilon)/(\mathsf{R}^{\mathsf{alt}}_{s,M}\mathsf{w}_s)$. Recall that $U_{\mathcal{A}^{\mathsf{alt}}\mathcal{B}}$ is designed such that the MASG flow (see (24)) matches the alternative electrical flow, per Theorem IV.5.

Hence by combining this with quantum amplitude estimation [64, 65], we obtain an ϵ-multiplicative estimate of p' at the cost of $O\left(\frac{1}{\epsilon}\log(\frac{1}{p'})\right)$ calls to the phase estimation routine.

The proof is concluded by modifying the quantum walk with the standard quantum walk technique that ensures that $\mathsf{R}^{\mathsf{alt}}_{s,M}\mathsf{w}_s = O(1)$, incuring an extra $\log(\mathsf{R}^{\mathsf{alt}}_{s,M}\mathsf{w}_s)$ (see [43, 44]) □

Once the alternative s-M electrical flow is forced to coincide with the MASG flow, we can estimate its energy, namely the quantity $\Phi(c_{s,M})$ defined in (25). Note that the quantity w_s in this case is equal to $\sum_{r\in\overrightarrow{\mathcal{R}}:s\in r}\nu_r\left|\nu_{r,s}\right|G_r$, which can be precomputed with the thermodynamical information stored in the (Q)RAM. For ease of notation however, we shall keep it abbreviated as w_s.

Corollary IV.8. *Fix an MAS $(\mathcal{S},\mathcal{C},\mathcal{R},k)$ that admits a detailed balance, that is particle conserving and whose underlying CRN is reversible. Fix an initial species s and a non-empty set of target species M and assume that the resulting MASG is s-M rigid. Then there exists a quantum walk algorithm that ϵ-multiplicatively estimates the instantaneous rate of Gibbs free–energy consumption $\Phi(c_{s,M})$ with a constant probability of success in cost*

$$O\left(\frac{1}{\epsilon}\left(\mathsf{S}+\frac{1}{\epsilon}\left(\mathsf{ET}^{\mathsf{alt}}_{s,M}+\log\left(\Phi(c_{s,M})\mathsf{w}_s\right)\right)\mathsf{U}^{\mathsf{alt}}_{\star}\right)\right).$$

Additionally, by employing Theorem IV.5, we can approximate, and subsequently sample from, the state

$$|\theta\rangle=\frac{1}{\sqrt{2\Phi(c_{s,M})}}\sum_{s\in\mathcal{S}}\sum_{r\in\overrightarrow{\mathcal{R}}}\frac{\theta_{s,r}}{\sqrt{\mathsf{w}_{s,r}}}\left(|s,r\rangle+|r,s\rangle\right).$$

Corollary IV.9. *Fix an MAS $(\mathcal{S},\mathcal{C},\mathcal{R},k)$ that admits a detailed balance, that is particle conserving and whose underlying CRN is reversible. Fix an initial species s and a non-empty set of target species M and assume that the resulting MASG is s-M rigid. Let θ be the MASG flow (see (24)). Then there exists a quantum walk algorithm that returns a state $|\widetilde{\theta}\rangle$ satisfying*

$$\frac{1}{2}\left\||\widetilde{\theta}\rangle\langle\widetilde{\theta}|-|\theta\rangle\langle\theta|\right\|\leq\epsilon$$

with a constant probability of success in cost

$$O\left(\mathsf{S}+\frac{1}{\epsilon^2}\left(\sqrt{\mathsf{ET}^{\mathsf{alt}}_{s,M}}+\log(\Phi(c_{s,M})\mathsf{w}_s)\right)\mathsf{U}^{\mathsf{alt}}_{\star}\right).$$

Additionally, we can return an ϵ-approximation of $J_r(c_{\sigma,M})^2/G_r$ for any $r\in\overrightarrow{\mathcal{R}}$ with a constant probability of success in cost

$$O\left(\frac{1}{\epsilon}\left(\mathsf{S}+\frac{1}{\epsilon^2}\left(\sqrt{\mathsf{ET}^{\mathsf{alt}}_{s,M}}+\log(\Phi(c_{s,M})\mathsf{w}_s)\right)\mathsf{U}^{\mathsf{alt}}_{\star}\right)\right).$$

Proof. The first part of the corollary follows directly from applying Theorem IV.5 with our modified quantum walk operator $U_{\mathcal{A}^{\mathsf{alt}}\mathcal{B}}$, ensuring that the MASG flow (see (24)) matches the alternative electrical flow.

For the second part, note that measuring the resulting state $|\widetilde{\theta}\rangle$ yields an edge adjacent to reaction r with a probability that is ϵ-multiplicatively approximate to

$$\frac{1}{\Phi(c_{s,M})} \sum_{s \in \mathcal{S}} \frac{\theta_{s,r}^2}{\mathsf{w}_{s,r}} = \frac{J_r(c_{\sigma,M})^2}{G_r}.$$

We can therefore approximate this quantity by applying quantum amplitude estimation. □

V. ACKNOWLEDGEMENTS

This work was supported by the Dutch National Growth Fund (NGF), as part of the Quantum Delta NL programme.

REFERENCES

[1]M. Feinberg, *Foundations of chemical reaction network theory* (Springer, 2019).

[2]M. Steiner and M. Reiher, Topics in Catalysis **65**, 6 (2022).

[3]J. Yang and R. Hu, The Astrophysical Journal **966**, 189 (2024).

[4]P. Loskot, K. Atitey, and L. Mihaylova, Frontiers in genetics **10**, 549 (2019).

[5]J. P. Unsleber and M. Reiher, Annual review of physical chemistry **71**, 121 (2020).

[6]P. L. Türtscher and M. Reiher, Journal of Chemical Information and Modeling **63**, 147 (2022).

[7]S. Stocker, G. Csanyi, K. Reuter, and J. T. Margraf, Nature communications **11**, 5505 (2020).

[8]J. P. Unsleber, S. A. Grimmel, and M. Reiher, Journal of Chemical Theory and Computation **18**, 5393 (2022).

[9]M. Wen, E. W. C. Spotte-Smith, S. M. Blau, M. J. McDermott, A. S. Krishnapriyan, and K. A. Persson, Nature Computational Science **3**, 12 (2023).

[10]Y. Liu, Y. Mo, and Y. Cheng, Industrial & Engineering Chemistry Research **64**, 5200 (2025).

[11]Z. G. Nicolaou, S. B. Nicholson, A. E. Motter, and J. R. Green, The Journal of Chemical Physics **158** (2023).

[12]M. Banaji, B. Boros, and J. Hofbauer, Applied Mathematics and Computation **426**, 127109 (2022).

[13]I. Ismail, R. Chantreau Majerus, and S. Habershon, The Journal of Physical Chemistry A **126**, 7051 (2022).

[14]M. P. Haag, A. C. Vaucher, M. Bosson, S. Redon, and M. Reiher, ChemPhysChem **15**, 3301 (2014).

[15]M. Bergeler, G. N. Simm, J. Proppe, and M. Reiher, Journal of chemical theory and computation **11**, 5712 (2015).

[16]J. Proppe, T. Husch, G. N. Simm, and M. Reiher, Faraday discussions **195**, 497 (2016).

[17]G. N. Simm and M. Reiher, Journal of chemical theory and computation **13**, 6108 (2017).

[18]G. N. Simm and M. Reiher, Journal of chemical theory and computation **14**, 5238 (2018).

[19]M. A. Heuer, A. C. Vaucher, M. P. Haag, and M. Reiher, Journal of chemical theory and computation **14**, 2052 (2018).

[20]G. N. Simm, A. C. Vaucher, and M. Reiher, The Journal of Physical Chemistry A **123**, 385 (2018).

[21]J. Proppe and M. Reiher, Journal of Chemical Theory and Computation **15**, 357 (2018).

[22]A. Baiardi, S. A. Grimmel, M. Steiner, P. L. Türtscher, J. P. Unsleber, T. Weymuth, and M. Reiher, Accounts of chemical research **55**, 35 (2021).

[23]M. Steiner and M. Reiher, Nature Communications **15**, 3680 (2024).

[24]C. H. Müller, M. Steiner, J. P. Unsleber, T. Weymuth, M. Bensberg, K.-S. Csizi, M. Mo¨rchen, P. L. Türtscher, and M. Reiher, The Journal of Physical Chemistry A **128**, 9028 (2024).

[25]K.-S. Csizi, M. Steiner, and M. Reiher, Nature Communications **15**, 5320 (2024).

[26]T. Weymuth, J. P. Unsleber, P. L. Türtscher, M. Steiner, J.-G. Sobez, C. H. Müller, M. Mörchen, V. Klasovita, S. A. Grimmel, M. Eckhoff, *et al.*, The Journal of Chemical Physics **160** (2024).

[27]M. Bensberg and M. Reiher, The Journal of Physical Chemistry A (2024).

[28]S. Habershon, The Journal of chemical physics **143** (2015).

[29]S. Habershon, Journal of Chemical Theory and Computation **12**, 1786 (2016).

[30]I. Ismail, H. B. Stuttaford-Fowler, C. Ochan Ashok, C. Robertson, and S. Habershon, The Journal of Physical Chemistry A **123**, 3407 (2019).

[31]I. Ismail, C. Robertson, and S. Habershon, The Journal of Chemical Physics **157** (2022).

[32]C. Robertson and S. Habershon, Catalysis Science & Technology **9**, 6357 (2019).

[33]C. Robertson, I. Ismail, and S. Habershon, ChemSystemsChem **2**, e1900047 (2020).

[34]Z. Fakhoury, G. C. Sosso, and S. Habershon, Journal of Chemical Information and Modeling **63**, 2181 (2023).

[35]Z. Fakhoury, G. C. Sosso, and S. Habershon, Journal of Chemical Theory and Computation **20**, 8340 (2024).

[36]J. T. Margraf and K. Reuter, ACS omega **4**, 3370 (2019).

[37]D. Doty and S. Zhu, Natural Computing **17**, 677 (2018).

[38]D. Doty and B. Heckmann, arXiv preprint arXiv:2405.08649 (2024).

[39]R. M. Alaniz, J. Brunner, M. Coulombe, E. D. Demaine, J. Diomidova, R. Knobel, T. Gomez, E. Grizzell, J. Lynch, A. Rodriguez, *et al.*, arXiv preprint arXiv:2303.15556 (2023).

[40]L. Einkemmer, J. Mangott, and M. Prugger, Journal of Computational Physics **503**, 112827 (2024).

[41]A. S. Perelson and G. F. Oster, Archive for Rational Mechanics and Analysis **57**, 31 (1974).

[42]F. Avanzini, N. Freitas, and M. Esposito, Physical Review X **13**, 021041 (2023).

[43]A. Belovs, arXiv preprint arXiv:1302.3143 (2013).

[44]S. Apers and S. Piddock, arXiv preprint arXiv:2211.16379 (2022).

[45]S. Jeffery and S. Zur, in *Proceedings of the 55th Annual ACM Symposium on Theory of Computing* (2023) pp. 1125–1130.

[46]S. Jeffery and G. Pass, in *42nd International Symposium on Theoretical Aspects of Computer Science (STACS 2025)* (Schloss Dagstuhl–Leibniz-Zentrum für Informatik, 2025) pp. 54–1.

[47]J. Li and S. Zur, Quantum **9**, 1733 (2025).

[48]C. Dürr, M. Heiligman, P. HOyer, and M. Mhalla, SIAM Journal on Computing **35**, 1310 (2006).

[49]G. A. Pavlopoulos, P. I. Kontou, A. Pavlopoulou, C. Bouyioukos, E. Markou, and P. G. Bagos, GigaScience **7**, giy014 (2018).

[50]A. Cornish-Bowden, *Fundamentals of enzyme kinetics* (John Wiley & Sons, 2013).

[51]L. A. Segel and M. Slemrod, SIAM review **31**, 446 (1989).

[52]E. Klipp, W. Liebermeister, C. Wierling, and A. Kowald, *Systems biology: a textbook* (John Wiley & Sons, 2016).

[53]S. R. De Groot and P. Mazur, *Non-equilibrium thermodynamics* (Courier Corporation, 2013).

[54]M. Szegedy, in *45th Annual IEEE symposium on foundations of computer science* (IEEE, 2004) pp. 32–41.

[55]F. Magniez, A. Nayak, J. Roland, and M. Santha, in *Proceedings of the thirty-ninth annual ACM symposium on Theory of computing* (2007) pp. 575–584.

[56]A. Ambainis, A. Gilyén, S. Jeffery, and M. Kokainis, in *Proceedings of the 52nd annual ACM SIGACT symposium on theory of computing* (2020) pp. 412–424.

[57]S. Apers, A. Gilyén, and S. Jeffery (2019).

[58]A. M. Childs, R. Cleve, E. Deotto, E. Farhi, S. Gutmann, and D. A. Spielman, in *Proceedings of the thirty-fifth annual ACM symposium on Theory of computing* (2003) pp. 59–68.

[59]S. Piddock, arXiv preprint arXiv:1912.04196 (2019).

[60]T. Ito and S. Jeffery, Algorithmica **81**, 2158 (2019).

[61]S. Jeffery, S. Kimmel, and A. Piedrafita, in *18th Conference on the Theory of Quantum Computation, Communication and Cryptography (TQC 2023)* (Schloss Dagstuhl-Leibniz-Zentrum für Informatik, 2023).

[62]A. Y. Kitaev, ECCC **TR96-003** (1996).

[63]A. Sakamoto, H. Kawakami, and K. Yoshikawa, Chemical physics letters **146**, 444 (1988).

[64]G. Brassard, P. Høyer, M. Mosca, and A. Tapp, Contemporary Mathematics **305**, 53 (2002).

[65]S. Fukuzawa, C. Ho, S. Irani, and J. Zion, in *2023 proceedings of the symposium on algorithm engineering and experiments (ALENEX)* (SIAM, 2023) pp. 135–147.

Appendix A: CRN models and assumptions

Chemical reaction networks (CRNs) can be mapped to graphs in several ways, each emphasizing different structural and computational aspects. Below we summarise three representative approaches.

Method 1: Energy–weighted reaction graphs. Reiher and co-workers pioneered graph-theoretical analyses of CRNs with an emphasis on quantum chemical accuracy [2, 5, 6, 8, 14–27]. Their work progressed from interactive visualization of reactivity to heuristics-guided searches, and later to error-controlled explorations using Gaussian process regression and spline-based interpolation of reaction paths. A central tool is *Pathfinder*, which encodes reactions as a weighted graph where edge weights reflect activation barriers or reaction costs. Shortest-path algorithms (e.g., Dijkstra, Yen) then identify kinetically accessible routes. While this enables automated discovery of multi-step mechanisms, limitations remain: kinetics are often simplified, accurate barrier data are essential, and scaling to large networks is computationally demanding. Future advances may rely on hybrid strategies combining quantum chemical methods, machine-learned potentials, and potentially quantum algorithms for shortest-path search, thereby improving scalability to chemically relevant networks.

Method 2: Connectivity-matrix (graph-of-graphs) representation. An alternative approach encodes each chemical species as a molecular graph, typically represented by a connectivity matrix (CM) [13, 28–35]. Reactions correspond to graph transformations—bond making/breaking events governed by predefined rules or templates. This reduces the exploration of chemical space to discrete transitions between connectivity patterns, each representing a stable (meta)structure. Random walks on this "graph-of-graphs" provide a stochastic but scalable strategy for pathway sampling, capable of revealing unexpected mechanisms (e.g., formaldehyde decomposition, Pt-catalyzed oxidation and aromatization). Refinement with dynamic reaction path sampling and graph-enforcing potentials integrates molecular dynamics while preserving connectivity constraints. Challenges include the neglect of conformational diversity, difficulty with proton-coupled processes, and exponential growth of connectivity states with molecular size.

Method 3: Bipartite molecule–reaction graphs. CRNs can also be represented as directed bipartite graphs [36], in which the vertex sets correspond to *molecules* and *reac-*

tions. Edges connect molecules to the reactions in which they participate, with directionality distinguishing reactants from products. Importantly, reversibility is naturally incorporated: reversing all edges of a reaction node does not invalidate the representation. This construction generalises to arbitrary stoichiometry and emphasises the indirect coupling of molecules via reactions, reminiscent of the "virtual flask" concept [17]. Bipartite graphs are particularly attractive for systematic enumeration of chemical subspaces, constraint-based modeling, and mapping to network-theoretic or quantum-inspired formalisms (e.g., bipartite matching, flow optimization, or Hamiltonian encodings for quantum algorithms).

In this work we adopt the bipartite representation as our baseline model, since it cleanly separates species and reactions and is naturally compatible with both graph-theoretical analysis and quantum algorithmic formulations.